Heliyon 10 (2024) e27393

Contents lists available at ScienceDirect

Heliyon

journal homepage: www.cell.com/heliyon

Research article

Compact MIMO UWB antenna integration with Ku band for advanced wireless communication applications

V.N. Koteswara Rao Devana [a], N. Radha [a], P. Sunitha [a], Fahad N. Alsunaydih [b], Fahd Alsaleem [b], Khaled Alhassoon [b,*]

[a] ECE Department, Aditya Engineering College, Surampalem, A.P, India
[b] Department of Electrical Engineering, College of Engineering, Qassim University, Buraydah, 52571, Saudi Arabia

ARTICLE INFO

Keywords:
Ku-band
MIMO
Smart electronics
UWB antenna
Wireless connectivity
IoT

ABSTRACT

This paper introduces a compact Multiple Input Multiple Output (MIMO) Ultrawideband (UWB) antenna seamlessly integrated with the Ku band, tailored for wireless communication applications. The MIMO antenna employs octagonal radiators, crafted from a tapered microstrip line-fed rectangular patch, etched on an economically efficient FR4 substrate measuring 40 × 23 mm^2. The octagonal configuration is achieved by introducing a rectangular patch to the central radiator, while parasitic stubs are strategically employed to mitigate coupling among MIMO elements. The antenna demonstrates an extensive operational bandwidth spanning 3.28–17.8 GHz, covering UWB, extended UWB, and Ku-band spectrums globally allocated for heterogeneous applications. With a peak gain of 4.93 dBi and an efficiency of 95.34%, the proposed MIMO antenna showcases superior performance. Key performance parameters, including a low envelope correlation coefficient (ECC) of 0.003 and a substantial diversity gain (DG) of 9.997 dB, are thoroughly analyzed. Comparative assessments against recent works validate the novelty and potential of the proposed antenna for integration into compact wireless systems. This study underscores the success of the antenna design in achieving a harmonious balance of compactness, wide operational bandwidth, and high performance, positioning it as a promising candidate for diverse wireless communication applications.

1. Introduction

Ultrawideband (UWB) technology has captivated the interest of a wide community of researchers due to the recent advancements made in wireless communication. UWB technology includes superior range and locating capabilities, excellent interoperability, enormous channel capacities, and low power consumption [1]. Initially, Primary focus is directed toward the filter designs for UWB as these filters play a crucial role in managing the wide spectrum of UWB signals, ensuring that only the desired frequencies are transmitted or received [2–4]. Afterward, additional endeavor was undertaken to design UWB antenna, ensuring uninterrupted transmission of the signals [5]. The UWB antennas have been in the business for the past several decades [6–8]. In 2002, the FCC proposed the band spectrum of 3.1–10.6 GHz for UWB applications [9]. After that, a lot of researchers started designing antennas for UWB applications [10–12]. The initial designs put more attention towards designing compact size antennas for covering whole UWB

* Corresponding author.
E-mail addresses: dvnkrao@gmail.com (V.N.K.R. Devana), radha.nainavarapu@aec.edu.in (N. Radha), sunithap@aec.edu.in (P. Sunitha), f.alsunaydih@qu.edu.sa (F.N. Alsunaydih), f.alsaleem@qu.edu.sa (F. Alsaleem), k.hassoon@qu.edu.sa (K. Alhassoon).

https://doi.org/10.1016/j.heliyon.2024.e27393
Received 12 January 2024; Received in revised form 23 February 2024; Accepted 28 February 2024
Available online 4 March 2024

spectrum. A microstrip and co-planar waveguide model of transmission line as well as reflector antennas and improving the bandwidth using complementary split ring resonator (CSRR) filters are common techniques utilized to design UWB antennas [13–15]. However, due to the emergence of the latest technologies and advancement in electronic systems there is a need for more efficient antennas.

A reconfigurable antenna possessing the capabilities to cover UWB, or limited band spectrum or selective bands could be utilized to nullify the aforementioned challenges [16–18]. Still these antennas can't be used for vast modern applications requiring a Multiple-Input-Multiple-Output (MIMO) antennas not limited to Wi-Fi, LTE, 5G new radio (NR) [19]. Along with that internet of things (IoT), Vehicular communication (V2V and V2X), wireless sensors networks and Point-to-point (P2P) communication [20–22]. Moreover, other band spectrums are also exploited for more applications including extended UWB spectrum utilized for real time location system, precision distance measurement, medical imaging and healthcare [23]. Along with that, Ku-band is also a widely studied frequency band spectrum that is allocated globally for satellite communication and radar system, fixed satellite services, maritime and aeronautical communication along with its application in remote sensing and high-frequency trading network [24]. Thus, a new demand arises in the research domain to design a smart antenna capable of possessing the feature of covering UWB, extended UWB and Ku-band spectrum along with MIMO functionality. Moreover, the additional feature of compact size and low mutual coupling among MIMO elements becomes critical for a modern-day communication system [25].

A number of works have been reported recently for extended UWB applications [26–34]. In Ref. [26] circular shaped two-port UWB MIMO antenna is presented with an overall size of 64 × 40 mm^2. A Y-shaped stubs is loaded along with ground plane to acvheive low mutual coupling of > -18 dB. Another circular shaped radiator based 2-port MIMO antenna is proposed in Ref. [27], where extended ground plane and parasitic stubs are loaded in the structure to achieve low mutual coupling. The wide band ranges 3–20 GHz is achieved with a setback of bigger physical size of 60 × 29.5 mm^2. A diagonally placed elements configuration is utilized in Ref. [28] along with grounded stubs to achieve UWB ranges 2–13 GHz while having coupling of > -17 dB. Likewise, orthogonal placement along with defected ground structure is utilized to achieve low coupled UWB antenna [29,30]. However, both works exhibit larger physical size along with coupling of > -15 dB that is not suitable for many applications. Relatively compact size MIMO antennas are presented in Refs. [31–33], however, they suffered from high coupling or have geometrically complex structure making it unsuitable for massive production.

Thus, there is a dire need for a UWB MIMO antenna offering wideband coverage ranges from UWB to Ku-band to mitigate the need of multiple antennas for various applications [34]. Therefore, this work proposed a compact antenna comprised of simple structure to cover band ranges from 3.28 GHz to 17.8 GHz. Moreover, the antenna offers coupling of > -20 dB by incorporating parasitic stubs loaded technique. The workflow of the rest of the manuscript is: In Section 2, the geometry of the MIMO element is discussed. In Section 3, the simulation-based parametric analysis of the MIMO-UWB antenna's DGS, feed structure and coupling element is presented. The functionality of the MIMO radiator is examined in Section 4, which includes associated discussions, simulations, and observed results.

2. MIMO antenna design

2.1. Antenna structure

Fig. 1(a and b) depicts the suggested UWB-MIMO antenna's geometry. The radiator is etched on a FR4 substrate with a ε_r of 4.40, a thickness of 1.6 mm, and δ of 0.02. The size of the radiator is $L_S \times W_S$ mm^2. The 50-Ω microstrip line with size $W_{F1} \times L_{F1}$ feeds both MIMO elements. A triangular tapered feed line is used for feeding the exponentially tapered feed region and patch of the proposed antenna. Tapered structures are employed so that the input signal to the antenna can radiate freely without any disturbance from the antenna. It has been observed experimentally that the antenna is well matched for a very broad frequency range [35,36]. Fig. 1 (a) shows how to achieve required impedance bandwidth by utilizing a tapered feed of dimension $W_{F2} \times L_{F2}$ mm^2 and the isolation of >17.25 dB is obtained by a split parasitic element. The MIMO antenna has a circular DGS that's having a radius 'R' mm as shown in Fig. 1 (b). Optimized parameters of proposed work are as follows: $W_S = 40$, $L_S = 23$, $d = 3.38$, $W_{F1} = 3$, $L_F = 8.5$, $W_{F2} = 1$, $L_{F1} = 0.5$, L_{F2}

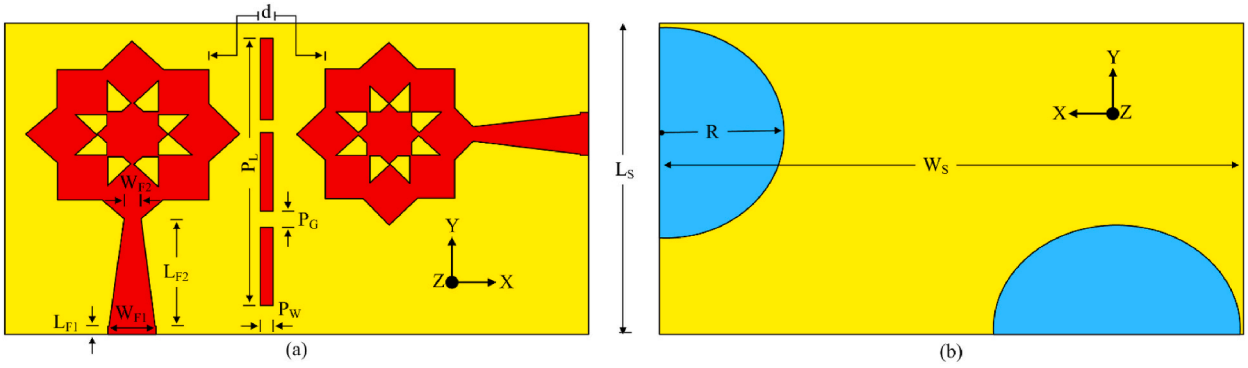

Fig. 1. Proposed MIMO antenna (a) top-view (b) back-view.

$= 8$, $P_L = 20$, $P_W = 1$, $P_G = 1$, $R = 8$, $\alpha = 45^0$.

2.2. Design methadology

The design methodology adopted to design a single element of MIMO antenna is shown in Fig. 2(a–j). The antenna design is extracted from a rectangular radiator which is then loaded with a fractal patch tilted at 45^0. Afterward, another fractal is loaded at the top end, as shown in Fig. 2 (Step-3). Similarly, another titled patch is loaded with a tilt angle of 45^0. In this way, fractal patches are loaded until the outer loop is completed, which results in UWB antenna. The loading of fractals results in achieving a wideband response. Hereafter, the unit element is copied and tilted orthogonally to form a 2-port MIMO antenna system. Finally, the antenna optimization is performed in 3 steps.

1) Truncating the ground plane.
2) Tapering the feeding line.
3) Parasitic patch to reduce coupling.

CST Studio Suite 2021 is utilized for the designing and optimization of the antenna. The optimization steps are discussed in detail to better understand the working of the proposed MIMO antenna.

2.3. Effect of defected ground structure

The optimization of the ground plane is carried out by following two major steps, as shown in Fig. 3(a–c). It was observed that with a rectangular ground plane the antenna is offering UWB ranges 5–18 GHz, as depicted in Fig. 4. However, there are few sub-bands inside the region where the impedance matching is quite low. Thus, to improve the impedance matching of the antenna, the upper corners of the ground plane are truncated using triangular slot, as exhibited in Fig. 3 (b). This iteration results in improved impedance matching at several frequencies; however, neither the operational band nor the sub-bands are improved. Therefore, instead of using triangular slots, a smoother cutting is performed so that the ground is shaped like a semi-circular structure, as depicted in Fig. 3 (c).

A semi-circular shaped partial ground plane enhances antenna bandwidth by minimizing reflections, improving impedance matching, and promoting a symmetrical radiation pattern. The curved design reduces discontinuities and edge effects, ensuring a more predictable and stable radiation pattern across the UWB spectrum. The gradual transition of resonant modes accommodates multiple frequencies, contributing to broader bandwidth [37]. Additionally, the semi-circular shape minimizes cross-polarization and supports consistent performance. When incorporated into UWB antenna designs, the semi-circular ground plane becomes a crucial element, influencing impedance characteristics and radiation patterns to achieve optimal performance over a wide range of frequencies [38,39]. This technique works effectively with the proposed structure and results shows that the impedance matching is improved throughout the band while the antenna offers a $|S_{11}| > -10$ dB bandwidth of 3.28–17.8 GHz, as shown in Fig. 4. It is important to note that not only ground plane but also the tapering of feedline helps to achieve the UWB behavior and discussed in later section.

2.4. Effects of tapered feeding

Another key parameter to control the bandwidth of the proposed MIMO antenna system is the feedline structure, as shown in Fig. 5.

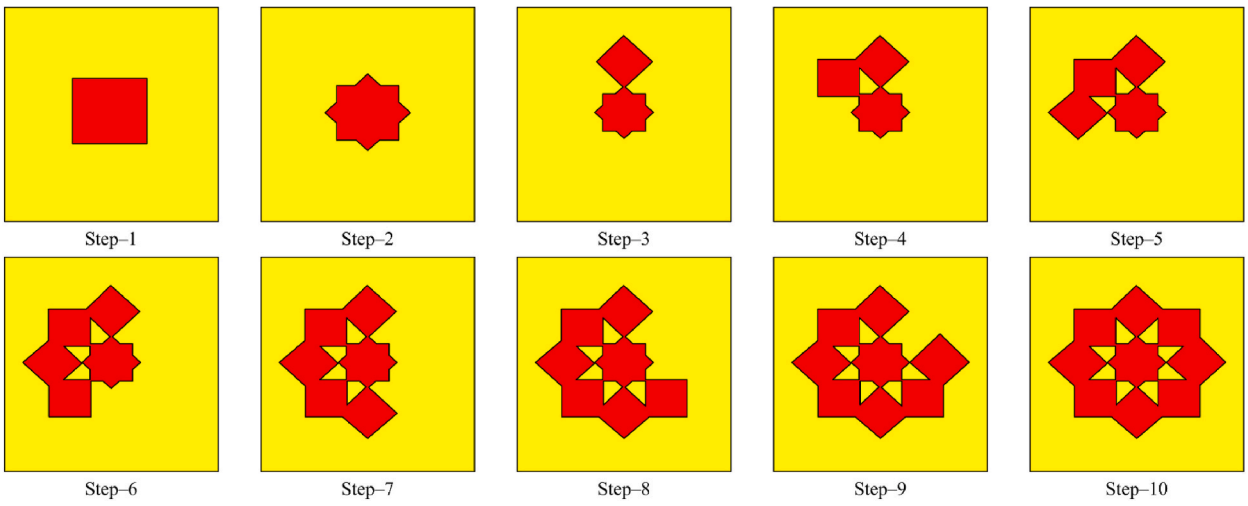

Fig. 2. Extraction steps of proposed antenna structure (a) step-1 (b) step-2 (c) step-3 (d) step-4 (e) step-5 (f) step-6 (g) step-7 (h) step-8 (i) step-9 (j) step-10.

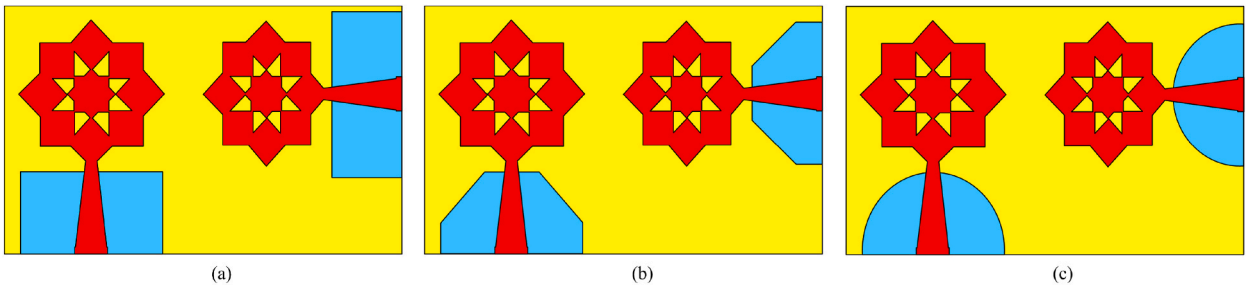

Fig. 3. Various modifications in ground structure (a) step-1 (b) step-2 (c) step-3.

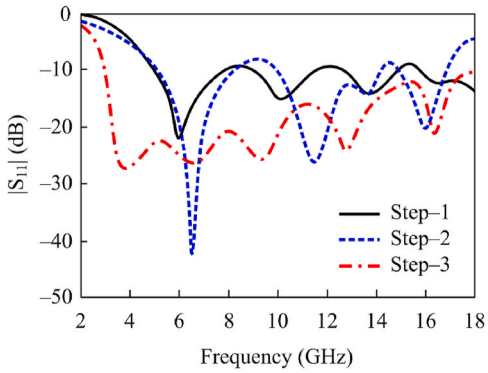

Fig. 4. Return loss of modification in ground structure.

In the pursuit of enhancing impedance bandwidth, tapering a feed line involves systematically altering the cross-sectional dimensions or electrical attributes of the transmission line along its length. By tapering, impedance mismatches and reflections are reduced, promoting smoother signal transmission. The gradual change in the feedline's characteristics allows for better impedance matching over a broader frequency range, contributing to increased bandwidth and improved overall antenna performance. The phenomenon is well observed in Fig. 6 where the antenna with conventional feedline offers a poor impedance matching over various frequencies in UWB region. However, when the tapering is done on feedline an improved impedance matching is observed over entire bandwidth. Thus, it can be concluded that the shape of ground plane plays an important role to control the impedance bandwidth range while the feedline controls the impedance matching in operational region.

2.5. Effects of decoupling stubs

Although an UWB is achieved by using two element MIMO antenna, the mutual coupling among the elements is high and thus not suitable for practical applications. Mutual coupling occurs when electromagnetic fields from one antenna affect the performance of adjacent antennas, leading to issues like reduced isolation and degraded system performance [40,41]. Therefore, more efforts have been made to reduce the mutual coupling; for the said purpose the open-ended parasitic stubs are utilized, as shown in Fig. 7(a–c). A

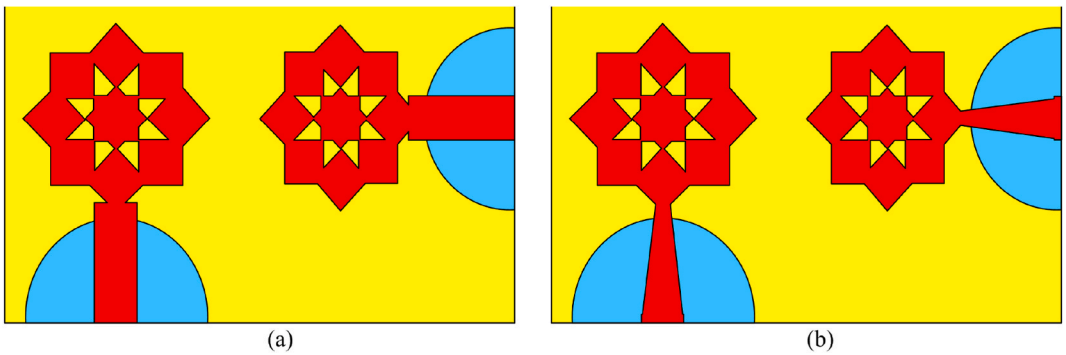

Fig. 5. Feedline modification steps (a) conventional (b) modified feed.

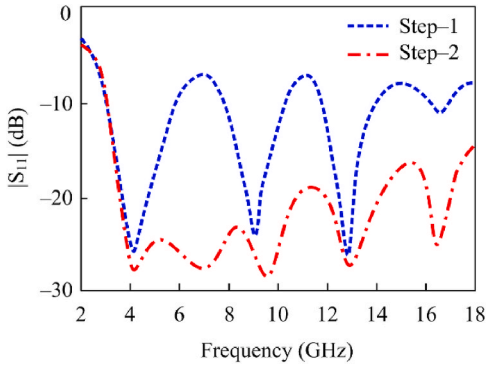

Fig. 6. Effects of impedance matching due to variation in feedline structure.

single parasitic stub can be strategically employed to reduce mutual coupling among MIMO antenna elements in wireless communication systems. Due to the low complexity of the structure, it is ideal choice for the aforementioned purpose, the position and thickness of the stub is optimized using parametric analysis. The optimized performance with single parasitic stub is shown in Fig. 8, where reduction in mutual coupling is observed over a wide range.

However, there is still room for improvement which results in utilization of multiple parasitic stubs instead of using single stubs. Multiple parasitic stubs are instrumental in mitigating mutual coupling among MIMO antenna elements in wireless communication systems. These stubs strategically positioned between antennas act as electromagnetic barriers, improving isolation and minimizing interference. By adjusting the length and position of the stubs, phase compensation is achieved, countering the effects of mutual coupling, and maintaining orthogonality between MIMO channels. Parasitic stubs also enable control over the radiation pattern, directing energy away from neighboring antennas. The frequency selectivity of the stubs contributes to better performance in multi-frequency MIMO systems. Compact and versatile, this design approach provides an effective means to enhance MIMO system reliability, particularly in applications with spatial constraints. The optimal placement of the stubs results in achievement of mutual coupling > -20 dB throughout the operational band, as depicted in Fig. 8.

3. Results and discussion

3.1. Fabricated prototype

To validate the outcomes of the proposed research, a sample prototype is manufactured through a chemical etching process. A commercially accessible 50-Ω SMA connector is soldered for excitation purposes, as illustrated in both the top and bottom views shown in Fig. 9(a and b). The fabrication of this prototype serves as a tangible verification of the theoretical findings, enabling a practical assessment of the proposed work's feasibility and functionality. The utilization of a standard 50-Ω SMA connector ensures compatibility and consistency in the excitation process, facilitating accurate comparisons between theoretical predictions and real-world results. This experimental validation is crucial for establishing the practical viability of the proposed work and confirming the alignment between theoretical modeling and physical implementation. Fig. 9(c) shows the far-field measurement setup inside the RF chamber.

3.2. Simulated and measured Reesults

The two-port MIMO antenna system exhibits commendable performance across a broad frequency range from 3.28 GHz to 17.8 GHz, as shown in Fig. 10 (a). This frequency range aligns with the demands of modern wireless communication systems, catering to various applications such as high-speed data transmission, radar systems, and emerging technologies within the specified spectrum.

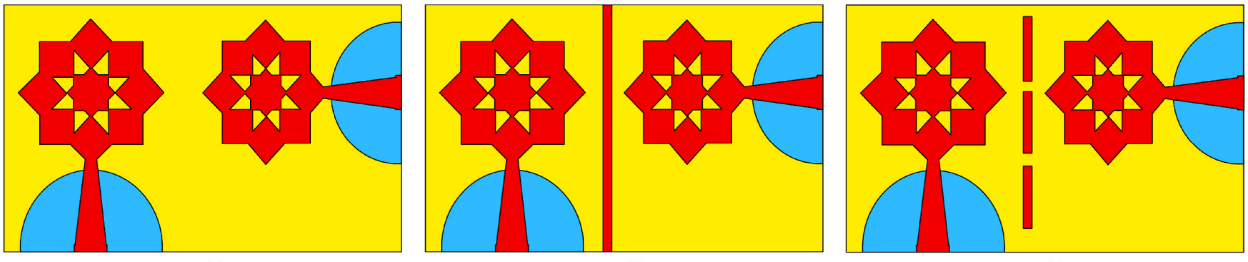

Fig. 7. Decoupling mechanism implementation stages (a) step-1 (b) step-2 (c) step-3.

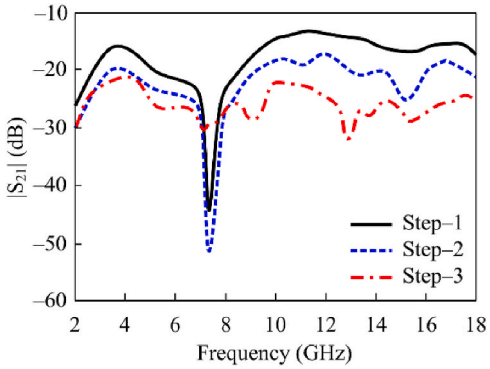

Fig. 8. Effects on coupling with and without parasitic stubs.

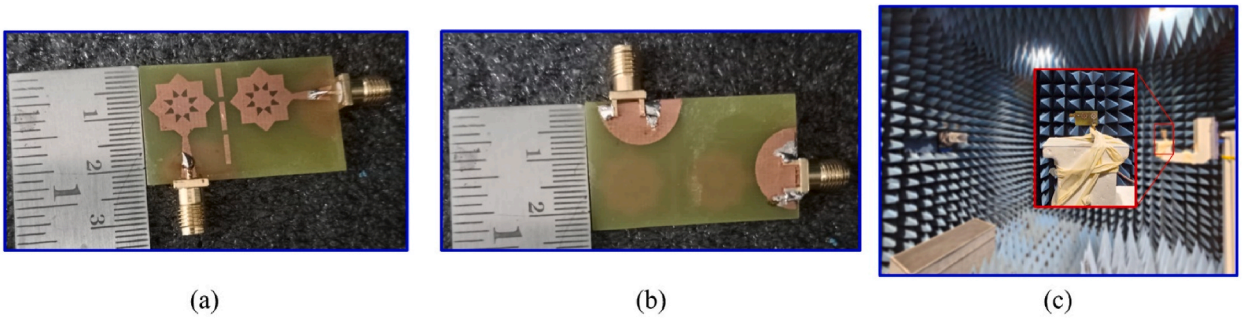

Fig. 9. Fabricated prototype of the proposed antenna (a) top–view (b) bottom–view (c) measurement setup.

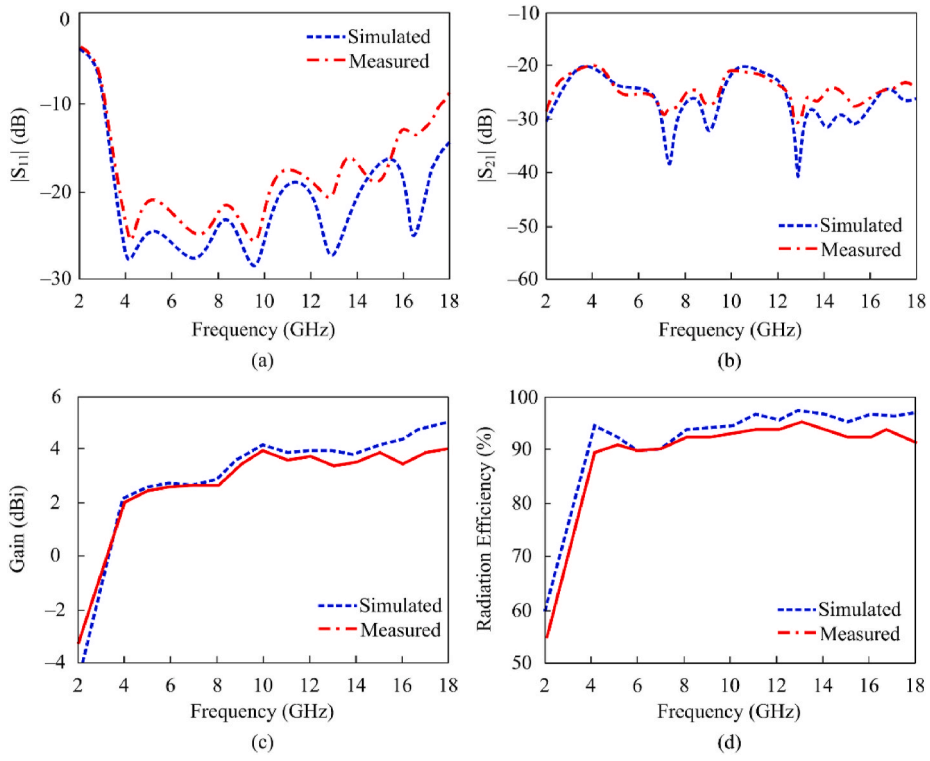

Fig. 10. Comparison among simulated and measured results (a) $|S_{11}|$ (b) $|S_{12}|$ (c) gain (d) radiation efficiency.

The design considerations and performance metrics of the MIMO antenna system are pivotal for ensuring reliable and efficient communication. One of the key metrics indicating the effectiveness of the MIMO antenna system is the achieved mutual coupling among its elements. Mutual coupling refers to the undesired electromagnetic interaction between adjacent antennas in a MIMO array. In this case, the mutual coupling is impressively below −20 dB, signifying a substantial reduction in the undesired electromagnetic coupling between the antenna elements when separated by 3.38 mm, as shown in Fig. 10 (b). This reduction is crucial for maintaining the independence of each antenna element, ensuring that the signals transmitted or received by one element do not unduly influence neighboring elements. Achieving a mutual coupling below −20 dB is indicative of a well-engineered design that minimizes interference and crosstalk between MIMO channels.

Moreover, the gain of the MIMO antenna system is reported to be greater than 2 dBi across the specified frequency range, as shown in Fig. 10 (c). Antenna gain represents the ability of the antenna to direct or concentrate the radiated energy in a specific direction. A gain exceeding 2 dBi indicates that the antenna system effectively amplifies the transmitted or received signals, contributing to improved communication range and link performance. This gain is especially significant in applications where signal strength and coverage are critical considerations. In addition to gain, another crucial performance metric is radiation efficiency. The MIMO antenna system achieves radiation efficiency exceeding 90%. Radiation efficiency is a measure of how effectively the electrical power supplied to the antenna is converted into radiated electromagnetic energy. A radiation efficiency exceeding 90% is indicative of an antenna system that minimizes losses and maximizes the conversion of electrical power into useful radiated signals, as exhibited in Fig. 10 (d). High radiation efficiency is desirable for optimizing the overall performance of the antenna system, ensuring that a significant portion of the input power is utilized for communication purposes.

Moreover, the reported measured results align closely with the simulated results, validating the accuracy and reliability of the antenna design. Consistency between simulated and measured results is a crucial aspect of antenna engineering, as it ensures that the theoretical models used in the design process accurately represent the real-world behavior of the antenna. The close agreement between simulation and measurement indicates that the design process, including the selection of materials, dimensions, and configurations, has been successful in achieving the intended performance characteristics.

In Fig. 11(a and b), the measured and simulated radiation patterns of the radiator are illustrated for both the E-plane and H-plane at frequencies of 4.12 GHz and 9.52 GHz, respectively. In the E-plane, the radiation patterns exhibit a bidirectional nature, indicating energy propagation predominantly along the axis perpendicular to the radiator's structure. Conversely, in the H-plane, the radiation patterns are nearly omnidirectional, suggesting a more uniform distribution of energy in a horizontal plane. The measured patterns closely align with the simulated ones, validating the accuracy of the theoretical predictions.

3.3. Diversity performance parameters

In the context of MIMO antenna systems, several key parameters and metrics play crucial roles in assessing their performance and efficiency. The ECC (Envelope Correlation Coefficient), DG (Diversity Gain), MEG (Mutual Coupling Effect on Gain), and Multiplexing Efficiency are discussed in this section.

ECC measures the correlation between the envelopes of signals received by different antenna elements in a MIMO system. It quantifies how closely the amplitudes of the received signals align. A low ECC indicates better diversity and less correlation, which is desirable for MIMO systems as it implies improved spatial separation and enhanced diversity gain. The ECC is estimated using the below formula provided in Ref. [42]:

$$ECC = \frac{|S_{11}{}^{*}S_{12} + S_{22}S_{21}{}^{*}|^{2}}{\left(1 - |S_{11}|^{2} - |S_{21}|^{2}\right)\left(1 - |S_{22}|^{2} - |S_{12}|^{2}\right)} \tag{1}$$

For proposed work the ECC of less than 0.002 is observed throughout the band of interest, as depicted in Fig. 12 (a). Another key parameter for MIMO performance analysis is diversity gain (DG). DG is a measure of how much the presence of multiple antennas improves the system's performance in terms of reducing fading and enhancing reliability. It is related to the ECC and represents the ratio of the diversity gain to that of a single antenna. A higher diversity gain signifies improved system performance in fading environments. The DG can be found in terms of ECC by using the following relation provided in Ref. [43]:

$$DG = 10\sqrt{1 - ECC^{2}} \tag{3}$$

Ideally the ECC should be zero, which results in DG of 10 dB, however, in practical application ECC have some value thus the DG never be equal to 10. The value closer to 10 dB is acceptable for DG and proposed work offers the DG of more than 9.9 dB, as depicted in Fig. 12 (b).

As the mutual coupling refers to the undesired interaction between antennas in a MIMO array. Mean Effective Gain (MEG) assesses how the gain of one antenna is affected by the presence of neighboring antennas. Excessive mutual coupling can lead to degradation in antenna performance and impact the radiation pattern and efficiency. The MEG can be estimated using the expression given in Refs. [44,45]. The value closer to -3dB is acceptable for MEG and the proposed work satisfied this criterion, as shown in Fig. 12 (c).

Lastly, multiplexing efficiency (ME) is a measure of how effectively a MIMO system utilizes its available spatial resources for simultaneous data transmission. It reflects the system's ability to transmit multiple data streams independently through different antenna elements. High multiplexing efficiency is desirable for achieving higher data rates in MIMO communication. A value closer to 0% is highly desirable for practical application. The comparison of simulated analysis of MIMO parameters and measured results offers a strong result proving the potential of the proposed work for targeted applications, as exhibited in Fig. 12 (d).

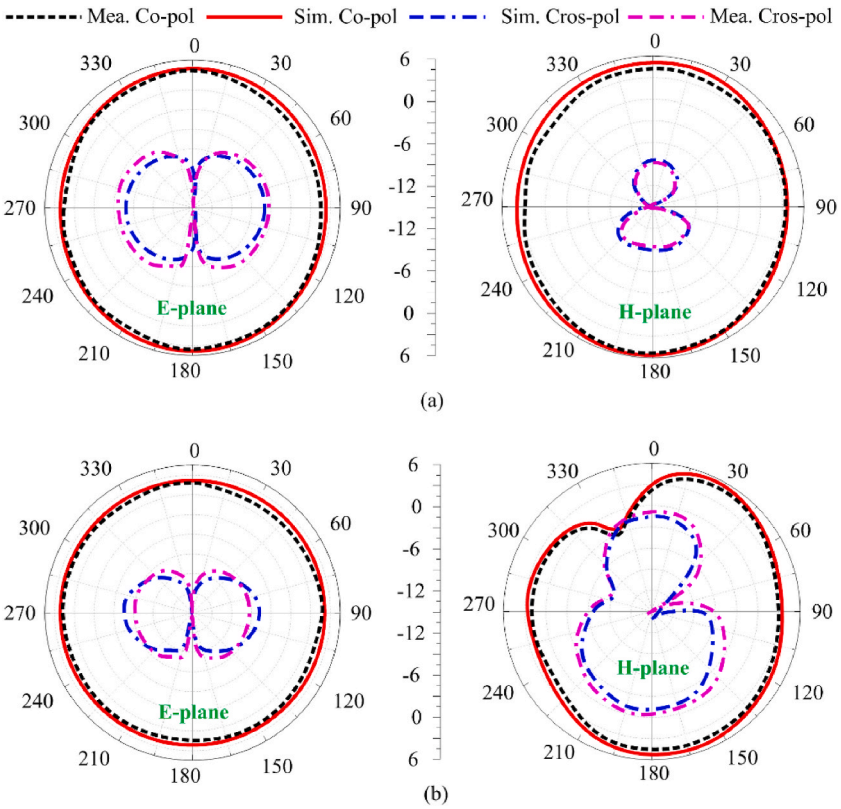

Fig. 11. Contrasting the simulated and measured radiation patterns at frequencies (a) 4.12 GHz and (b) 9.52 GHz.

The comparison of the proposed work with similar related work is carried out in Table 1. The proposed work offers compact size as compared to rest of the works, except [34] where the size is more compact at the cost of high mutual coupling. Moreover, proposed work covers a wider bandwidth as compared to most of the works. Work reported in Ref. [27] offers a much wider bandwidth while posing larger physical size as compared to proposed work along with having a setback of high coupling. Thus, it can be derived that proposed work overperforms the literary work and becomes a stronger candidate for UWB, extended wideband and Ku-band application requiring MIMO system.

4. Conclusions

In conclusion, this paper presents a groundbreaking compact Multiple Input Multiple Output (MIMO) Ultrawideband (UWB) antenna seamlessly integrated with the Ku band, catering to wireless communication applications. The MIMO antenna features octagonal radiators, achieved through the integration of a rectangular patch into the central radiator. The use of a tapered microstrip line and parasitic stubs effectively reduces coupling among MIMO elements. Fabricated on an economical FR4 substrate with dimensions of 40 $\times$ 23 mm^2, the antenna showcases an extensive operational bandwidth spanning 3.28–17.8 GHz, covering UWB, extended UWB, and Ku-band spectrums, aligning with global allocations for heterogeneous applications. With a peak gain of 4.93 dBi and an impressive efficiency of 95.34%, the proposed MIMO antenna exhibits superior performance. In-depth analysis of MIMO parameters reveals a low envelope correlation coefficient (ECC) of 0.003 and a remarkable diversity gain (DG) of 9.997 dB. Comparative assessments with recent works validate the novelty and potential of this proposed antenna for integration into compact wireless systems. The findings highlight the success of the antenna design in achieving a harmonious blend of compactness, wide operational bandwidth, and high performance, making it a promising candidate for diverse wireless communication applications.

Data availability statement

Data included in article/supp. Material/referenced in article.

CRediT authorship contribution statement

V.N. Koteswara Rao Devana: Writing – original draft, Software, Resources, Conceptualization. **N. Radha:** Writing – original draft, Software, Resources, Conceptualization. **P. Sunitha:** Writing – original draft, Software, Resources, Conceptualization. **Fahad N.**

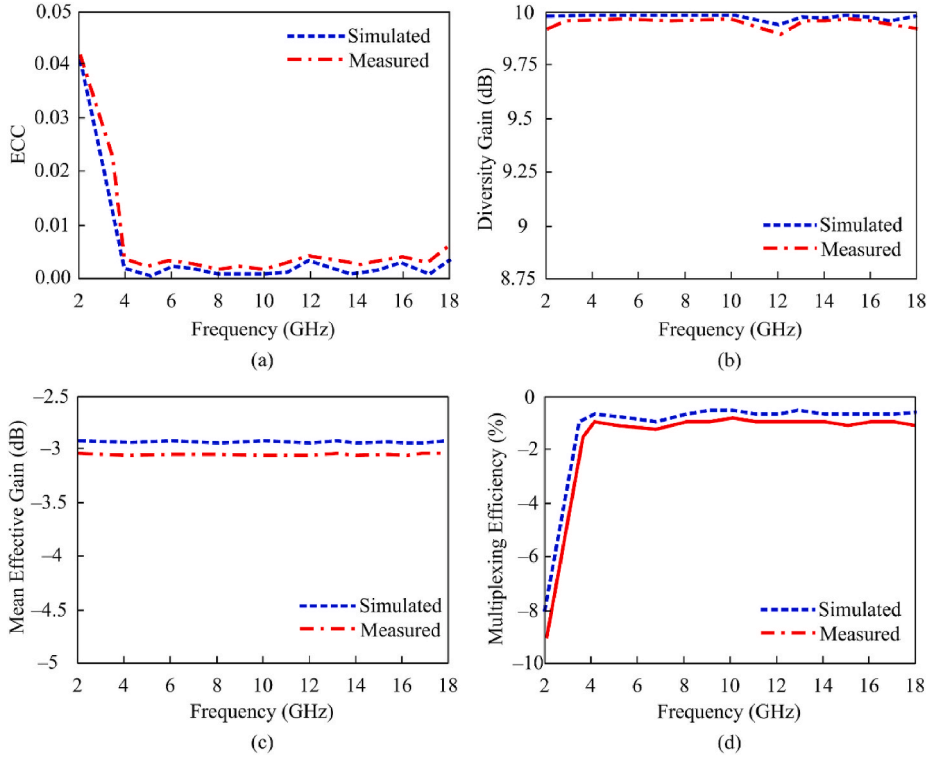

Fig. 12. Comparison among simulated and measured diversity parameters (a) ECC (b) DG (c) MEG (d) Mul. Eff.

Table 1
Comparison of proposed work with literature work.

Ref.	Size (mm^2)	Bandwidth (GHz)	Mutual coupling (dB)	Isolation method
[26]	64 × 40	3–13	< −18	Grounded stub
[27]	40 × 22	1.42–2.52	< −15	Grounded and parasitic stubs
[28]	46 × 46	2.3–13	< −17	Defected ground structure
[29]	40 × 40	3–11	< −15	Grounded stub
[30]	40 × 40	3–13.5	< −15	Defected ground structure
[31]	60 × 35	3.1–10.6	< −15	Parasitic stubs
[32]	30 × 45	3–11	< −20	Defected ground structure
[33]	38.5 × 38.5	3.08–11.8	< −15	Defected ground structure
[34]	40 × 22	3.18–11.26	< −15	Parasitic stubs
Prop.	40 × 23	3.28–17.8	< −20	Parasitic stubs

Alsunaydih: Writing – review & editing, Methodology, Investigation, Formal analysis, Data curation. **Fahd Alsaleem:** Writing – review & editing, Validation, Project administration. **Khaled Alhassoon:** Writing – review & editing, Validation, Supervision, Funding acquisition.

Declaration of competing interest

The authors declare that they have no known competing financial interests or personal relationships that could have appeared to influence the work reported in this paper.

Acknowledgment

Researchers would like to thank the Deanship of Scientific Research, Qassim University, for funding the publication of this project.

References

[1] K. Zhao, M. Zhu, B. Xiao, X. Yang, C. Gong, J. Wu, Joint RFID and UWB technologies in intelligent warehousing management system, IEEE Internet Things J. 7 (12) (2020) 11640–11655.

[2] B. Xu, Y. Guo, A novel DVL calibration method based on robust invariant extended Kalman filter, IEEE Trans. Veh. Technol. 71 (9) (2022) 9422–9434.
[3] X. Huang, X. Zhang, L. Zhou, J.X. Xu, J.F. Mao, Low-loss self-packaged Ka-band LTCC filter using artificial multimode SIW resonator, IEEE Transactions on Circuits and Systems II: Express Briefs 70 (2) (2023) 451–455.
[4] X.L. Huang, L. Zhou, J.F. Mao, Modified FSIW filter with *N* transmission zeros using BCB-based MEMS technology, IEEE Microw. Wireless Compon. Lett. 29 (8) (2019) 520–522.
[5] C. Wen, Y. Huang, L. Zheng, W. Liu, T.N. Davidson, Transmit waveform design for dual-function radar-communication systems via hybrid linear-nonlinear precoding, IEEE Trans. Signal Process. 71 (2023) 2130–2145.
[6] W.A. Awan, A. Zaidi, N. Hussain, A. Iqbal, A. Baghdad, Stub loaded, low profile UWB antenna with independently controllable notch-bands, Microw. Opt. Technol. Lett. 61 (11) (2019) 2447–2454.
[7] A. Abbas, N. Hussain, M.-J. Jeong, J. Park, K.S. Shin, T. Kim, N. Kim, A rectangular notch-band UWB antenna with controllable notched bandwidth and centre frequency, Sensors 20 (2020) 777.
[8] A. Zaidi, W.A. Awan, A. Ghaffar, M.S. Alzaidi, M. Alsharef, D.H. Elkamchouchi, S.S.M. Ghoneim, T.E.A. Alharbi, A low profile ultra-wideband antenna with reconfigurable notch band characteristics for smart electronic systems, Micromachines 13 (2022) 1803.
[9] S.N.R. Rizvi, W.A. Awan, N. Hussain, Design and characterization of miniaturized printed antenna for UWB communication systems, Journal of Electrical Engineering & Technology 16 (2021) 1003–1010.
[10] V.L.N. Phani Ponnapalli, S. Karthikeyan, J. Lakshmi Narayana, V.N. Koteswara Rao Devana, A compact SE-DGS tapered-fed notched UWB antenna integrated with Ku/K band for Breast Cancer Detection, IETE J. Res. (2023), https://doi.org/10.1080/03772063.2023.2185308.
[11] M. Hussain, T. Islam, M.S. Alzaidi, D.H. Elkamchouchi, F.N. Alsunaydih, F. Alsaleem, K. Alhassoon, Single iterated fractal inspired UWB antenna with reconfigurable notch bands for compact electronics, Heliyon 9 (11) (2023) 21419.
[12] V.N. Koteswara Rao Devana, Annaram Sowjanya, A. Beno, Vella Satyanarayana, B. Kiranmai, L. Siva Sai, B Kiran Kumar, A compact SWB-CSF antenna for Millimetre Wave wireless applications, J. Infrared, Millim. Terahertz Waves 43 (2022) 514–526.
[13] K.L. Chung, H. Tian, S. Wang, B. Feng, G. Lai, Miniaturization of microwave planar circuits using composite microstrip/coplanar-waveguide transmission lines, Alex. Eng. J. 61 (11) (2022) 8933–8942.
[14] Q. Wang, P. Li, P. Rocca, R. Li, G. Tan, N. Hu, W. Xu, Interval-based tolerance analysis method for petal reflector antenna with random surface and deployment errors, IEEE Trans. Antenn. Propag. 71 (11) (2023) 8556–8569.
[15] X. Huang, Design of miniaturized SIW filter loaded with improved CSRR structures, Electronics 12 (18) (2023) 3789.
[16] T. Islam, E.M. Ali, W.A. Awan, M.S. Alzaidi, T.A. Alghamdi, M. Alathbah, A parasitic patch loaded staircase shaped UWB MIMO antenna having notch band for WBAN applications, Heliyon 10 (2023) 23711.
[17] W.A. Awan, A. Zaidi, M. Hussain, N. Hussain, I. Syed, The design of a wideband antenna with Notching characteristics for small devices using a Genetic Algorithm, Mathematics 9 (2021) 2113.
[18] A. Li, C. Masouros, A.L. Swindlehurst, W. Yu, 1-bit massive MIMO transmission: Embracing interference with symbol-level precoding, IEEE Commun. Mag. 59 (5) (2021) 121–127.
[19] R. Chataut, R. Akl, Massive MIMO systems for 5G and beyond networks—overview, recent trends, challenges, and future research direction, Sensors 20 (10) (2020) 2753.
[20] H. Min, Y. Li, X. Wu, W. Wang, L. Chen, X. Zhao, A measurement scheduling method for multi-vehicle cooperative localization considering state correlation, Vehicular Communications 44 (2023) 100682.
[21] H. Xu, S. Han, X. Li, Z. Han, Anomaly Traffic Detection based on communication-efficient Federated Learning in Space-Air-ground integration network, IEEE Trans. Wireless Commun. 22 (12) (2023) 9346–9360.
[22] H. Min, X. Lei, X. Wu, Y. Fang, S. Chen, W. Wang, X. Zhao, Toward Interpretable Anomaly Detection for Autonomous Vehicles with Denoising Variational Transformer, Engineering Applications of Artificial Intelligence, 2024 107601.
[23] S. Emami, UWB Communication Systems: Conventional and 60 GHz, Springer, New York, 2016.
[24] S.C. Ho, R. Shah, J.L. Garrison, P.N. Mohammed, A. Schoenwald, R. Pannu, J.R. Piepmeier, Wideband ocean altimetry using Ku-band and K-band satellite signals of opportunity: proof of concept, Geosci. Rem. Sens. Lett. IEEE 16 (7) (2019) 1012–1016.
[25] X. Chen, S. Zhang, Q. Li, A review of mutual coupling in MIMO systems, IEEE Access 6 (2018) 24706–24719.
[26] M.K. Sharma, M. Kumar, J.P. Saini, S. Sukla, N. Bhati, UWB-MIMO diversity antenna for next generation wireless applications, in: 2016 3rd International Conference on Computing for Sustainable Global Development, INDIACom), 2016, pp. 1528–1532.
[27] V.N. Koteswara Rao Devana, G. Asa Jyothi, Savanam Chandrasekhar, V.L.N. Phani Ponnapalli, N. G Sekhar Reddy, Radha. A Compact MIMO Antenna for GPS/PCS/Bluetooth Wireless Applications. 2023 3rd International Conference on Intelligent Technologies, 2023.
[28] W.A. Ali, A.A. Ibrahim, A compact double-sided MIMO antenna with an improved isolation for UWB applications, AEU-International Journal of Electronics and Communications 82 (2017) 7–13.
[29] A.A. Khan, S.A. Naqvi, M.S. Khan, B. Ijaz, Quad port miniaturized MIMO antenna for UWB 11 GHz and 13 GHz frequency bands, AEU-International Journal of Electronics and Communications 131 (2021) 153618.
[30] V.N. Koteswara Rao Devana, A. Maheswara Rao, An octagonal shaped MIMO UWB antenna with dual band notched characteristics. Intelligent communication technologies and Virtual Mobile networks ICICV 2019, Lecture Notes on Data Engineering and Communications Technologies 33 (2020) 599–606.
[31] J.Y. Deng, L.X. Guo, X.L. Liu, An ultrawideband MIMO antenna with a high isolation, IEEE Antenn. Wireless Propag. Lett. 15 (2015) 182–185.
[32] L. Kang, H. Li, X. Wang, X. Shi, Compact offset microstrip-fed MIMO antenna for band-notched UWB applications, IEEE Antenn. Wireless Propag. Lett. 14 (2015) 1754–1757.
[33] V.N. Koteswara Rao Devana, A. Maheswara Rao, A novel dual band notched MIMO UWB antenna, Progress In Electromagnetics Research Letters 93 (2020) 65–71.
[34] V.N. Koteswara Rao Devana, A. Maheswara Rao, A compact flower slotted dual band notched ultrawideband antenna integrated with Ku band for ultrawideband, medical, direct broadcast service, and fixed satellite service applications, Microw. Opt. Technol. Lett. 63 (2) (2021) 556–563.
[35] M. Manohar, R.S. Kshetrimayum, A.K. Gogoi, Printed monopole antenna with tapered feed line, feed region and patch for super wideband applications, IET Microw., Antennas Propag. 8 (1) (2013) 39–45.
[36] Venkata Naga Koteswara Rao Devana; Emandi Kusuma Kumari; Karnam Serkadu Chakradhar; Purnima Kadali Sharma, Danthuluri Rama Devi, Chebrolu Manohar Kumar, Valluri Dhana Raj, Devathoti Rajendra Prasad, A novel foot-shaped elliptically embedded patch-ultra wide band antenna with quadruple band notch characteristics verified by characteristic mode analysis, Int. J. Commun. Syst. 35 (15) (2022) e5284.
[37] E.M. Ali, W.A. Awan, M.S. Alzaidi, A. Alzahrani, D.H. Elkamchouchi, F. Falcone, S.S.M. Ghoneim, A shorted stub loaded UWB flexible antenna for small IoT devices, Sensors 23 (2023) 748.
[38] W.A. Awan, M. Alibakhshikenari, E. Limiti, A Poly-Di-Methyl-Siloxane Based Conformal Ultra-wideband Antenna with Additional GSM Band. 2021 IEEE Asia-Pacific Microwave Conference, APMC), 2021, pp. 67–69.
[39] W.A. Awan, S.I. Naqvi, A. Ghaffar, On the design of PDMS based miniaturized ultra-wideband antenna for compact flexible electronics, in: 2022 IEEE International Symposium on Antennas and Propagation and USNC-URSI Radio Science Meeting, AP-S/URSI), 2022, pp. 595–596.
[40] Y. Jiang, S. Liu, M. Li, N. Zhao, M. Wu, A new adaptive co-site broadband interference cancellation method with auxiliary channel, Digital Communications and Networks (2022).
[41] M.K.A. Jannat, M.S. Islam, S. Yang, H. Liu, Efficient Wi-Fi-based human activity recognition using adaptive antenna elimination, IEEE Access 11 (2023) 105440–105454.
[42] N. Hussain, W.A. Awan, W. Ali, S.I. Naqvi, A. Zaidi, T.T. Le, Compact wideband patch antenna and its MIMO configuration for 28 GHz applications, AEU-International Journal of Electronics and Communications 132 (2021) 153612.

[43] H. Zahra, W.A. Awan, W.A.E. Ali, N. Hussain, S.M. Abbas, S. Mukhopadhyay, A 28 GHz broadband Helical inspired end-Fire antenna and its MIMO configuration for 5G pattern diversity applications, Electronics 10 (2021) 405.
[44] J. Jung, W.A. Awan, D. Choi, J. Lee, N. Hussain, N. Kim, Design of high-gain and low-mutual-coupling multiple-input–multiple-Output antennas based on PRS for 28 GHz applications, Electronics 12 (2023) 4286.
[45] V.K.R. Devana, A. Beno, M.S. Alzaidi, P.B.M. Krishna, G. Divyamrutha, W.A. Awan, T.A.H. Alghamdi, M. Alathbah, A high bandwidth dimension ratio compact super wide band-flower slotted microstrip patch antenna for millimeter wireless applications, Heliyon 10 (2023) 23712.